# Acceptance angle for Bragg reflection of atoms from a standing light wave

Stephan Dürr and Gerhard Rempe
*Fakultät für Physik, Universität Konstanz, 78457 Konstanz, Germany*
(Received 24 June 1998)

We experimentally investigate Bragg reflection of atoms from a standing light wave. We focus on the influence of small angular deviations from the exact Bragg resonance onto the reflection probability. The Bragg resonance has a finite acceptance angle, which depends on the light intensity. Within this acceptance angle, an oscillatory behavior of the reflection probability as a function of the angle is observed.
[S1050-2947(99)02302-1]

PACS number(s): 03.75.Be, 32.80.−t, 42.50.Vk

Bragg reflection of atoms from a standing light wave is a useful tool in atom optics, because it makes possible to realize a coherent beam splitter for atoms with only two output beams. After Bragg reflection had been demonstrated in several experiments during the last decade [1–4], it has recently been employed in atom interferometers [5,6]. For Bragg reflection to occur, the atomic beam must enter the standing light wave at a Bragg angle. It is obvious that for small angular deviations from the exact resonance the probability of Bragg reflection is still nonzero, i.e., there is a finite acceptance angle. How large is it? So far, this acceptance angle has not been studied in atom optics experiments [7,8]. However, recent experiments with a new atom interferometer [6] rely on a detailed investigation of this acceptance angle. We find that it is proportional to the light intensity, and that the reflection probability oscillates as a function of the angle for small deviations from the exact resonance. The experimental results are in good agreement with a simple theoretical model, which we present before discussing the experiment.

## THEORETICAL MODEL

We apply the theoretical model discussed in Refs. [9–15] to the specific situation of our experiment. In atom optics, the Bragg angle is typically very small, i.e., the incoming atomic beam is nearly perpendicular to the wave vector of the light. This allows us to make a Fresnel approximation. We choose a coordinate system with the $z$ axis parallel to the wave vector of the light and with the $x$ axis nearly parallel to the atomic beam. In the Fresnel approximation the longitudinal atomic momentum $p_x$ is treated classically and is assumed to be unaffected by the light. Only the $z$ coordinate has to be treated quantum mechanically.

For Bragg reflection, the angle of incidence $\vartheta$ fulfills the condition $2d\sin\vartheta = N\lambda_{\rm dB}$. Here $d$ is the spatial period of the light intensity and equals half a light wavelength, $d=\lambda_{\rm light}/2$. The atomic de Broglie wavelength, $\lambda_{\rm dB}=h/p$, is determined by the atomic momentum $p$, and $N$ is the order of reflection, which is an integer. The Bragg condition can be rewritten as a condition for the transverse atomic momentum $p_z = p\sin\vartheta$, yielding $p_z = N\hbar k$, where $k=2\pi/\lambda_{\rm light}$ is the wave vector of the light.

We treat the atom as a two-level system and assume that the light frequency is sufficiently far detuned from the atomic resonance, so that excitation and spontaneous emission can be neglected. Hence the atom experiences only a conservative potential, the so-called ac-Stark shift: $V(z) = 4\hbar\chi\cos^2(kz)$. The potential depth is determined by the ac-Stark shift parameter $\chi = R^2/(4\Delta)$, which depends on the peak traveling-wave Rabi frequency $R$ and the atom-light detuning $\Delta = \omega_{\rm light} - \omega_{\rm atom}$. With this potential the Hamiltonian in the Fresnel approximation is

$$H(z) = -\frac{\hbar^2}{2m}\frac{\partial^2}{\partial z^2} + 4\hbar\chi\cos^2(kz). \tag{1}$$

We assume that the initial atomic state is a plane wave with transverse momentum $p_z$, which we normalize with respect to the photon momentum $\hbar k$, by writing

$$p_z = n\hbar k. \tag{2}$$

The corresponding momentum state is denoted by $|n\rangle$. If $n$ happens to be an integer then the Bragg condition is fulfilled. However, we do not require $n$ to be an integer, in order to investigate the effect of deviations from the exact Bragg angle. Using $\cos^2(kz) = \{2+\exp(-2ikz)+\exp(2ikz)\}/4$, we find

$$H|n\rangle = \hbar\omega_{\rm rec}n^2|n\rangle + \hbar\chi\{2|n\rangle + |n-2\rangle + |n+2\rangle\}, \tag{3}$$

where $\omega_{\rm rec} = \hbar k^2/(2m)$ is the recoil frequency. The term $2\hbar\chi|n\rangle$ in Eq. (3) represents a constant energy shift, equal for all momentum states. We can drop this term by choosing an appropriate interaction picture, resulting in

$$H|n\rangle = \hbar\omega_{\rm rec}n^2|n\rangle + \hbar\chi\{|n-2\rangle + |n+2\rangle\}. \tag{4}$$

This equation shows that the light couples momentum states with a momentum difference of $2\hbar k$. This can easily be explained because a standing wave consists of two counterpropagating traveling waves. An atom can absorb a photon out of one of these traveling waves followed by an induced emission into the other traveling wave. This Raman-like two-photon process transfers two photon momenta to the atom.

We focus on first-order Bragg-reflection, i.e., $n\approx 1$. In order to investigate the acceptance angle, we include small deviations from the exact resonance,

$$n = 1 + \Delta n \quad \text{with} \quad |\Delta n| \ll 1. \tag{5}$$

 

According to Eq. (4), the initially populated momentum state $|1+\Delta n\rangle$ is coupled to states $\{\ldots,|-3+\Delta n\rangle,|-1+\Delta n\rangle,|1+\Delta n\rangle,|3+\Delta n\rangle,\ldots\}$. While the states $|-1+\Delta n\rangle$ and $|1+\Delta n\rangle$ are nearly degenerate, the kinetic energies of the states $|3+\Delta n\rangle$ and $|1+\Delta n\rangle$ differ by $\approx 8\hbar\omega_{\rm rec}$. We consider the case of weak coupling, i.e., $|\chi|\ll 8\omega_{\rm rec}$, where this mismatch between the kinetic energies prevents the transfer of significant population to the state $|3+\Delta n\rangle$. A similar argument applies to the state $|-3+\Delta n\rangle$. This allows us to perform a two-beam approximation, i.e., we neglect the coupling to all momentum states, except $|-1+\Delta n\rangle$ and $|1+\Delta n\rangle$. In a matrix representation with respect to the states $\{|-1+\Delta n\rangle,|1+\Delta n\rangle\}$ the Hamiltonian is

$$H=\hbar\begin{pmatrix}(-1+\Delta n)^2\omega_{\rm rec} & \chi \\ \chi & (1+\Delta n)^2\omega_{\rm rec}\end{pmatrix}. \qquad (6)$$

This matrix contains the kinetic energies of the momentum states in the diagonal elements and the light-induced coupling between the states in the off-diagonal elements.

We assume that the light intensity is turned on instantaneously at time $t=0$, stays constant during the interaction, and is turned off instantaneously at time $t=\tau$. With the initial condition $|\psi(t=0)\rangle=|1+\Delta n\rangle$, we can define the amplitude coefficients $c_T$ and $c_R$ for transmission and reflection by

$$|\psi(t=\tau)\rangle=c_T|1+\Delta n\rangle+c_R|-1+\Delta n\rangle. \qquad (7)$$

They fulfill $|c_T|^2+|c_R|^2=1$. Using the Hamiltonian in Eq. (6), the Schrödinger equation can easily be solved, yielding the reflection probability

$$|c_R|^2=\frac{1}{1+\left(2\frac{\omega_{\rm rec}}{\chi}\Delta n\right)^2}\times\frac{1}{2}\left[1-\cos\{\tau\sqrt{(2\chi)^2+(4\omega_{\rm rec}\Delta n)^2}\}\right]. \qquad (8)$$

For $\Delta n=0$, Eq. (8) predicts a sinusoidal oscillation of $|c_R|^2$ as a function of $\tau$ (or $\chi$), which is called *Pendellösung* [16]. For fixed $\chi$ and $\tau$, $|c_R|^2$ also oscillates as a function of $\Delta n$. The first factor in Eq. (8) is a Lorentzian envelope for this oscillation, describing the finite acceptance angle for Bragg reflection. The full width at half maximum (FWHM) of this Lorentzian is

$$\Delta n_L=\chi/\omega_{\rm rec}. \qquad (9)$$

This width is proportional to the light intensity, but independent of the interaction time $\tau$, so that the behavior is more similar to power broadening than to interaction time broadening. The number of oscillation periods within $\Delta n_L$ increases with increasing $\chi\tau$.

Similar calculations have been performed for the so-called Laue case in Bragg reflection of x rays [16] or neutrons [17] from solid-state crystals. In these cases the typical Bragg angles are large, so that the Fresnel approximation cannot be performed, and the calculations are more complicated. However, similar features have been predicted, namely, a Lorentzian envelope and an oscillation for angular deviations from the exact resonance. This oscillation has been observed experimentally with x rays [18] and neutrons [19], but not with atoms.

## EXPERIMENTAL RESULTS

The experiment is performed with the apparatus described in Ref. [20]. $^{85}$Rb atoms are loaded into a magneto-optical trap (MOT). After trapping and cooling, the cloud of atoms is released and falls freely through the apparatus. The resulting pulsed atomic beam is collimated with a mechanical slit 20 cm below the MOT. The atoms then pass the interaction region with the standing light wave. The interaction time $\tau$ of the atoms with the standing light wave is controlled by switching the light on and off. This allows us to create a rectangular pulse shape, as assumed in the above calculation. In the far field of the interaction region, 45 cm below the MOT, the atomic position distribution is observed by exciting the atoms with a resonant laser beam and detecting the fluorescence photons. This far-field position distribution represents the atomic momentum distribution after the interaction with the standing light wave. As compared to Ref. [20] only a few changes have been made: the width of the collimation slit was enlarged to 450 $\mu$m; in order to improve the position resolution, the horizontal waist of the detection laser beam was reduced to $\omega=50$ $\mu$m, and a second collimation slit with a width of 100 $\mu$m was added 1 cm below the MOT. The standing light wave has a vertical waist of $\omega=10$ mm. This gives rise to an angular uncertainty in the direction of the photons [1] of 12 $\mu$rad, which is negligible.

Figure 1 shows the atomic far-field position distribution after Bragg reflection from the standing light wave. Atoms in the right half of the figure have been transmitted, atoms in the left half have been Bragg reflected. The dashed line shows an envelope that consists of two broad peaks. The shape of the right peak is determined by the collimation slits. It is the measured distribution of atoms without Bragg reflection. The left peak is a Bragg-reflected image of the right peak. The system is aligned so that the Bragg resonance, $\Delta n=0$, is found in the middle of each peak. The momentum width of the incoming atomic beam corresponds to $\Delta n\approx 0.5$ (FWHM). The data were recorded for $\chi/\omega_{\rm rec}=1.0$, 0.5, 0.3, and 0.15 in parts (a), (b), (c), and (d), respectively ($\omega_{\rm rec}=2\pi\times 3.8$ kHz). Here, we are not primarily interested in observing the *Pendellösung* oscillations. Hence we keep the probability of reflection at $\Delta n=0$ fixed by tuning the interaction time $\tau$ in such a way that $2\chi\tau=\pi$. Each solid line in Fig. 1 shows a fit to the theoretical expectation based on Eq. (8). The shapes of the fit curves are in good agreement with the experimental data. For $2\chi\tau=\pi$, the oscillation of the reflection probability as a function of $\Delta n$ is strongly suppressed by the Lorentzian envelope and, therefore, hardly visible. Note that an angular deviation of, e.g., $\Delta\vartheta=1$ mrad corresponds to $\Delta n=0.33$ and to a displacement of $\Delta z=0.55$ mm in the detector plane.

Figure 2 shows the best-fit values for the width of the Lorentzian envelope $\Delta n_L$, which determines the acceptance angle for Bragg reflection. The solid line in Fig. 2 shows the theoretical expectation from Eq. (9), which is in good agreement with the experimental data. Only for very small values of $\chi$ the measured value of $\Delta n_L$ is limited by the position

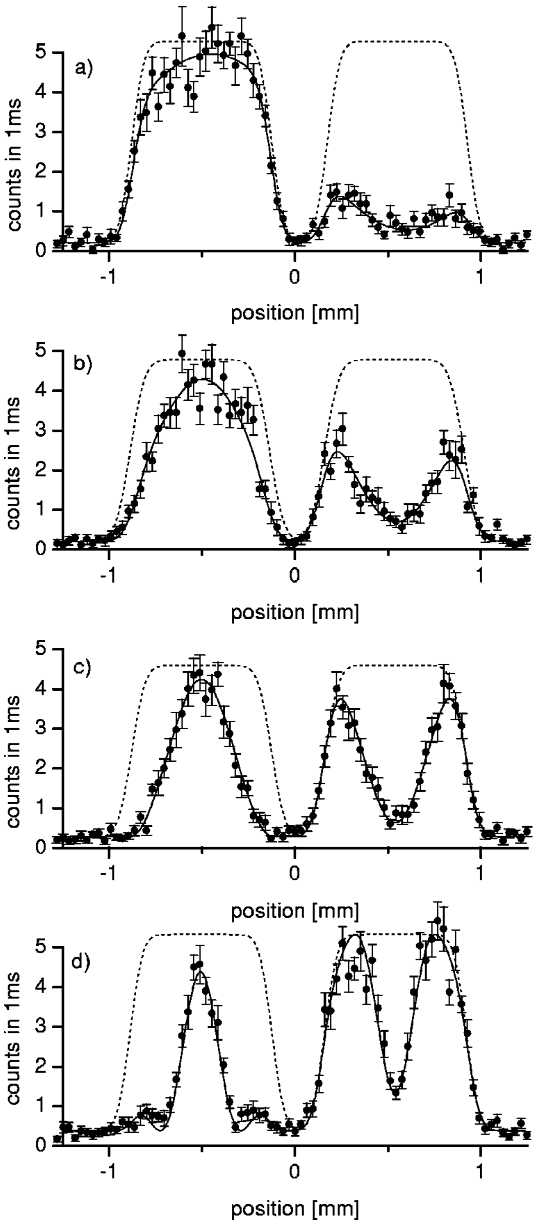


FIG. 1. Far-field position distribution of atoms after Bragg reflection from a standing light wave. Atoms on the left have been first-order Bragg reflected, while atoms on the right have been transmitted. The dashed line shows the envelope, as explained in the text. Each solid line is a fit to the theoretical expectation based on Eq. (8). The acceptance angle for Bragg reflection is tuned by varying the intensity of the standing light wave. In parts (a), (b), (c), and (d) the ac-Stark shift parameter $\chi$ is tuned to $\chi/\omega_{\rm rec}=1.0$, 0.5, 0.3, and 0.15, respectively. In all these measurements, $2\chi\tau=\pi$.

resolution of the apparatus. Both axes in Figure 2 have been calibrated by independent measurements. Measurements for $\chi/\omega_{\rm rec}\gg 1$ would not be useful, because the two-beam approximation would not be justified in this regime.

We now turn to the oscillatory behavior for angular deviations from the exact Bragg resonance. Fig. 3 shows the far-field position distribution of reflected atoms. Only reflected atoms are shown, corresponding to the left half of Fig. 1. On the horizontal axis, the labels give the transverse momentum $\Delta n$, which corresponds to the far-field position. The dashed lines show the same envelope as in Fig. 1. The

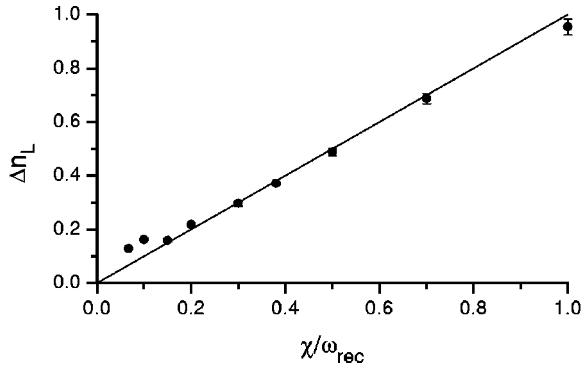


FIG. 2. Acceptance angle for Bragg reflection. The width of the Lorentzian envelope $\Delta n_L$ is shown as a function of the ac-Stark shift parameter $\chi$. Each data point is obtained from a fit to a data set like those shown in Fig. 1. The solid line is the theoretical expectation from Eq. (9).

alignment of the system was changed, so that the middle of the peak now corresponds to $\Delta n \approx 0.25$. The data were recorded with $\chi = 0.6\omega_{\rm rec}$. In parts (a), (b), and (c) we chose $\tau=105$ $\mu$s, 210 $\mu$s, and 330 $\mu$s yielding $2\chi\tau\approx\pi, 2\pi$, and $3\pi$, respectively. Hence the reflection probability at $\Delta n=0$

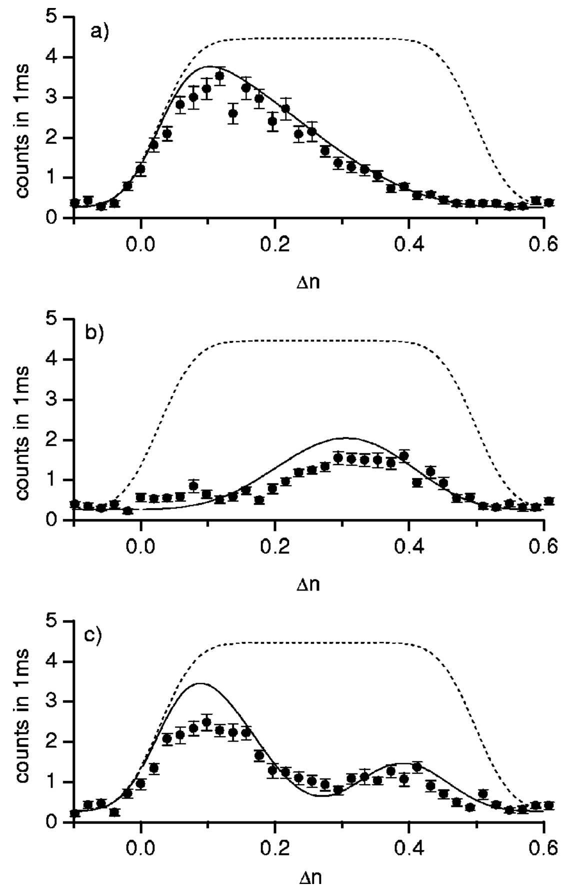


FIG. 3. Diffraction pattern of atoms after Bragg reflection from a standing light wave. Only reflected atoms are shown, corresponding to the left peak in Fig. 1. The reflection probability oscillates as a function of the deviation $\Delta n$ of the transverse momentum from the exact Bragg resonance. Parts (a), (b), and (c) were recorded with $2\chi\tau=\pi, 2\pi$ and $3\pi$, respectively, while $\chi$ was set to $0.6\omega_{\rm rec}$. The solid line shows the theoretical expectation (see text).

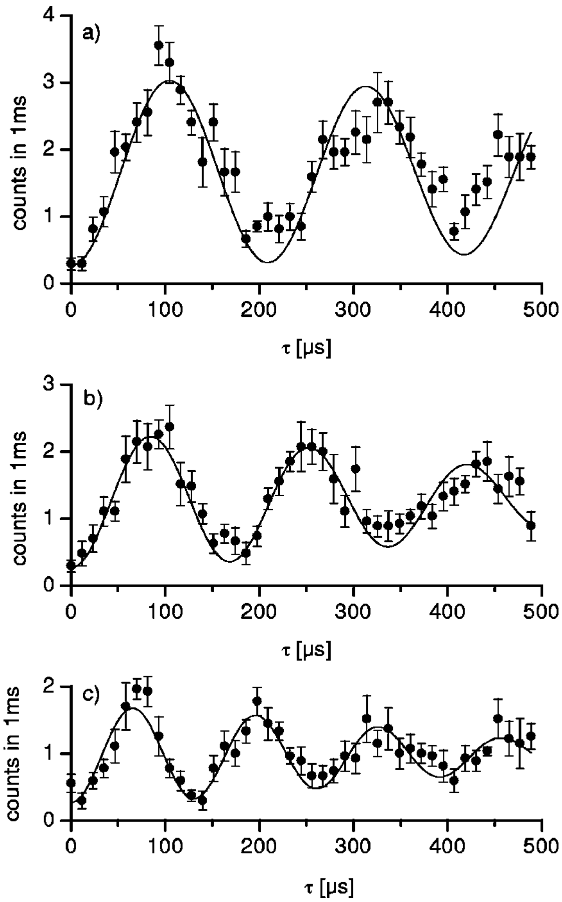


FIG. 4. *Pendellösung* as a function of the interaction time $\tau$ for a constant value of $\chi=0.6\omega_{\rm rec}$. The *Pendellösung* frequency depends on $\Delta n$. Parts (a), (b), and (c) are recorded at $\Delta n=0.1$, 0.25, and 0.4, respectively. The solid line shows the theoretical expectation (see text).

should be one in parts (a) and (c), and zero in part (b). The solid lines show the theoretical expectation, which is based on Eq. (8). We also take into account that the finite position resolution of the apparatus reduces the fringe visibility.

We now give a physical interpretation for this oscillation. For that purpose, we return to Eq. (6). This equation shows the Hamiltonian of a two-level system. Hence the behavior of the system is analogous to that of a two-level atom without spontaneous emission driven by a light field. The off-diagonal elements $\chi$ correspond to half the on-resonance Rabi frequency $R/2$, and the difference between the diagonal elements $4\omega_{\rm rec}\Delta n$ corresponds to the atom-light detuning $\Delta$. For a two-level atom the effective Rabi frequency is $\sqrt{R^2+\Delta^2}$, which should be compared with the *Pendellösung* frequency $\sqrt{(2\chi)^2+(4\omega_{\rm rec}\Delta n)^2}$, see Eq. (8).

Figure 4 displays the reflection probability, $|c_R|^2$, as a function of $\tau$ for $\chi=0.6\omega_{\rm rec}$ and three different angles, corresponding to $\Delta n=0.1$, 0.25, and 0.4 in parts (a), (b), and (c), respectively. The solid lines show the theoretical expectation based on Eq. (8). The increase of the *Pendellösung* frequency with increasing $\Delta n$ is in quantitative agreement with the theory. The *Pendellösung* is damped with increasing $\tau$, because an increase of $\tau$ creates narrower fringes in Fig. 3, which are washed out due to the finite position resolution. The solid lines in Fig. 4 take this effect into account. Finally, the decreasing amplitude of the *Pendellösung* with increasing $\Delta n$ is due to the Lorentzian envelope in Eq. (8).

We point out that the $\Delta n$ dependence of the reflection probability in Eq. (8) depends critically on the temporal shape of the light pulse. In particular, for a smooth pulse shape, a different envelope is obtained, and oscillations as a function of $\Delta n$ do not occur [11]. For such a smooth pulse, the width of the envelope is interaction-time broadened, i.e., proportional to $1/\tau$, but independent of the light intensity.

In conclusion, we have investigated the finite acceptance angle for Bragg reflection of atoms and the oscillation of the reflection probability for small angular deviations from the exact resonance. The scheme discussed here can be generalized to the case where the standing light wave is created by two traveling waves at slightly different frequencies. This shifts the Bragg resonance in momentum space, because the difference between the photon energies must now be compensated by a difference between the kinetic energies of the initial and the final momentum state [4,21]. Such a technique makes possible to address arbitrary momentum classes at will. The width of the addressed momentum class is determined by the acceptance angle for Bragg reflection. This technique finds applications in the preparation and diagnostics of atomic beams, as has already been demonstrated, e.g., in Raman-cooling experiments [22].

## ACKNOWLEDGMENTS

The authors acknowledge help from Axel Kuhn, Stefan Kunze, and Thomas Nonn. This work was supported by the Deutsche Forschungsgemeinschaft.

[1] P. J. Martin, B. G. Oldaker, A. H. Miklich, and D. E. Pritchard, Phys. Rev. Lett. **60**, 515 (1988).
[2] D. M. Giltner, R. W. McGrown, and S. A. Lee, Phys. Rev. A **52**, 3966 (1995).
[3] S. Kunze, S. Dürr, and G. Rempe, Europhys. Lett. **34**, 343 (1996).
[4] S. Bernet *et al.*, Phys. Rev. Lett. **77**, 5160 (1996).
[5] D. M. Giltner, R. W. McGrown, and S. A. Lee, Phys. Rev. Lett. **75**, 2638 (1995).
[6] S. Dürr, T. Nonn, and G. Rempe, Nature (London) **395**, 33 (1998).
[7] C. S. Adams, M. Sigel, and J. Mlynek, Phys. Rep. **240**, 145 (1994).
[8] *Atom Interferometry*, edited by P. R. Berman (Academic Press, New York, 1997).
[9] A. F. Bernhardt and B. W. Shore, Phys. Rev. A **23**, 1290 (1981).
[10] D. E. Pritchard and P. Gould, J. Opt. Soc. Am. B **2**, 1799 (1985).
[11] A. P. Kazantsev, G. I. Surdutovick, and V. P. Yakovlev, *Mechanical Action of Light on Atoms* (World Scientific, London, 1990).

[12] M. Wilkens, E. Schumacher, and P. Meystre, Phys. Rev. A **44**, 3130 (1991).
[13] E. Schumacher, M. Wilkens, P. Meystre, and S. Glasgow, Appl. Phys. B: Photophys. Laser Chem. **54**, 451 (1992).
[14] M. Marte and S. Stenholm, Appl. Phys. B: Photophys. Laser Chem. **54**, 443 (1992).
[15] S. Dürr, S. Kunze, and G. Rempe, Quantum Semiclassic. Opt. **8**, 531 (1996).
[16] P. P. Ewald, Ann. Phys. (Leipzig) **54**, 519 (1917).
[17] H. Rauch and D. Petrascheck, in *Neutron Diffraction*, edited by H. Dachs, Topics in Current Physics Vol. 6 (Springer, New York, 1978), pp. 303–351.
[18] U. Bonse, W. Graeff, R. Teworte, and H. Rauch, Phys. Status Solidi A **43**, 487 (1977).
[19] U. Bonse, W. Graeff, and H. Rauch, Phys. Lett. **69A**, 420 (1979).
[20] S. Kunze *et al.*, J. Mod. Opt. **44**, 1863 (1997).
[21] M. B. Dahan *et al.*, Phys. Rev. Lett. **76**, 4508 (1996).
[22] C. S. Adams and E. Riis, Prog. Quantum Electron. **21**, 1 (1997).